

# Theory of spin excitations and the microwave response of cylindrical ferromagnetic nanowires

Rodrigo Arias

*Departamento de Física, Universidad de Chile, Santiago, Chile*

D. L. Mills

*Department of Physics and Astronomy, University of California, Irvine, California 92697*

(Received 11 September 2000; published 16 March 2001)

We develop the theory of exchange/dipole spin wave excitations of ferromagnetic nanowires of cylindrical cross section, where the magnetization is parallel to the axis of the wire. In addition, we provide the theory of the microwave response of such structures, for the case where the nanowire is also a conductor. We present explicit calculations of both the mode structure of nanowires, and also their ferromagnetic resonance spectrum, with attention to recent experimental studies. We compare differences between the physical picture appropriate for the cylinder, with the well studied case of the ferromagnetic film.

DOI: 10.1103/PhysRevB.63.134439

PACS number(s): 75.30.Ds, 76.50.+g, 77.84.-s

## I. INTRODUCTION

In recent years, very considerable attention has been devoted to the study of ultrathin ferromagnetic films, and magnetic multilayers formed from such films. Such systems have unique physical properties, by virtue of the fact that a large fraction of the magnetic ions reside in low symmetry sites at the film surfaces, thus providing strong anisotropies not found in bulk magnetic matter constructed from the same ions. Also, in multilayers, exchange couplings between nearest neighbor films provide for diverse magnetic phases, spin reorientation transitions induced by very modest applied magnetic fields, and other phenomena as well. Finally, important applications of magnetic multilayers have been realized, and more are envisioned.

Other forms of magnetic nanostructures can be fabricated and studied as well. For example, Ebels and Wigen<sup>1</sup> have created arrays of very long ferromagnetic nanowires of Ni, permalloy and Co, with diameters in the range of 30 to 500 nm. These are very uniform in cross section, with lengths in the range of 20 microns. They thus are realizations of nanowires one can reasonably view as infinite in length, to excellent approximation. These authors have carried out ferromagnetic resonance studies of their samples, which consist of nanowire arrays, with individual entities accurately parallel to each other, but arranged randomly over a plane.

The diameter range explored in these studies is such that when one considers the spin wave modes of an isolated nanowire, it is necessary to include both exchange and dipolar contributions to their excitation energy. The present paper presents the theory of such dipole/exchange spin wave modes of isolated ferromagnetic nanowires of circular cross section, for the case where the magnetization is parallel to the symmetry axis of the wire. In addition, we provide a description of the ferromagnetic resonance absorption spectrum, for the case where, as in the samples discussed above, the materials are metallic in nature. It is thus important to take into account the influence of the finite skin depth, particularly for the larger diameters explored in these particular studies.

There is a long history of the study of the magnetostatic

spin wave modes of uniformly magnetized ferromagnets of various shapes,<sup>2</sup> with explicit attention to cylindrical samples.<sup>3</sup> However, little attention has been devoted to the inclusion of exchange, since these early studies were motivated by applications to ferrite samples of rather large dimensions. The structure of the spin wave modes accessible to microwave excitation in such samples are influenced little by exchange. In the particular case of samples of cylindrical shape, one study of the exchange dipole modes has appeared;<sup>4</sup> so far as we know, the text is not available in English, so its content is of limited accessibility.

There are two interesting implications of the mode structure of the ferromagnetic nanowires. First, as we shall see below, at long wavelengths, the dispersion is controlled by the long ranged dipolar fields. While details are different, very much as in ultrathin films,<sup>5,6</sup> the dipolar contribution can produce downward curvature in the dispersion relation at long wavelengths. At larger wave vectors, the curvature is always positive, as a consequence of the presence of exchange. Thus, one realizes short wavelength spin-wave modes degenerate in frequency with the uniform mode of the cylinder excited in ferromagnetic resonance. If the cylinder surfaces are not perfectly smooth, the two magnon dipolar mechanism operative in ultrathin films<sup>6,7</sup> should then also be "active" in the ferromagnetic nanowires. This will lead to extrinsic contributions to the ferromagnetic resonance linewidth similar to those demonstrated to be substantial in ultrathin ferromagnetic films.<sup>7</sup>

Also, when the ferromagnetic resonance mode of the nanowire is excited, the precession of the magnetization leads to large magnetic fields outside the sample, in contrast to the case of thin films, where the field is confined to the film interior. There should then be strong interactions between nanowires, in dense arrays such as those explored by Ebels and Wigen.<sup>1</sup> The consequence of these interactions is not explored here, though our formal structure can be used for this purpose.

In the discussion above, we have discussed on the experimental studies of Ebels and Wigen.<sup>1</sup> It should be remarked that Demokritov and Hillebrands<sup>8</sup> have carried out extensive studies of nanowire arrays. Their nanowires have rectangular

## Report Documentation Page

*Form Approved*  
OMB No. 0704-0188

Public reporting burden for the collection of information is estimated to average 1 hour per response, including the time for reviewing instructions, searching existing data sources, gathering and maintaining the data needed, and completing and reviewing the collection of information. Send comments regarding this burden estimate or any other aspect of this collection of information, including suggestions for reducing this burden, to Washington Headquarters Services, Directorate for Information Operations and Reports, 1215 Jefferson Davis Highway, Suite 1204, Arlington VA 22202-4302. Respondents should be aware that notwithstanding any other provision of law, no person shall be subject to a penalty for failing to comply with a collection of information if it does not display a currently valid OMB control number.

1. REPORT DATE <b>16 MAR 2001</b>	2. REPORT TYPE <b>N/A</b>	3. DATES COVERED <b>-</b>	
4. TITLE AND SUBTITLE <b>Theory of Spin Excitations and the Microwave Response of Cylindrical Ferromagnetic Nanowires</b>		5a. CONTRACT NUMBER <b>DAAD19-02-1-0174</b>	
		5b. GRANT NUMBER	
		5c. PROGRAM ELEMENT NUMBER	
6. AUTHOR(S)		5d. PROJECT NUMBER	
		5e. TASK NUMBER	
		5f. WORK UNIT NUMBER	
7. PERFORMING ORGANIZATION NAME(S) AND ADDRESS(ES) <b>Departamento de Fisica, Universidad de Chile, Santiago Chile</b>		8. PERFORMING ORGANIZATION REPORT NUMBER	
9. SPONSORING/MONITORING AGENCY NAME(S) AND ADDRESS(ES) <b>U.S. Army Research Office P.O. Box 12211 Research Triangle Park, NC 27709-2211</b>		10. SPONSOR/MONITOR'S ACRONYM(S)	
		11. SPONSOR/MONITOR'S REPORT NUMBER(S) <b>42253.15-PH</b>	
12. DISTRIBUTION/AVAILABILITY STATEMENT <b>Approved for public release, distribution unlimited</b>			
13. SUPPLEMENTARY NOTES			
14. ABSTRACT <b>We develop the theory of exchange/dipole spin wave excitations of ferromagnetic nanowires of cylindrical cross section, where the magnetization is parallel to the axis of the wire. In addition, we provide the theory of the microwave response of such structures, for the case where the nanowire is also a conductor. We present explicit calculations of both the mode structure of nanowires, and also their ferromagnetic resonance spectrum, with attention to recent experimental studies. We compare differences between the physical picture appropriate for the cylinder, with the well studied case of the ferromagnetic film.</b>			
15. SUBJECT TERMS			
16. SECURITY CLASSIFICATION OF:			17. LIMITATION OF ABSTRACT <b>SAR</b>
a. REPORT <b>unclassified</b>	b. ABSTRACT <b>unclassified</b>	c. THIS PAGE <b>unclassified</b>	
			18. NUMBER OF PAGES <b>12</b>
			19a. NAME OF RESPONSIBLE PERSON

cross section, however. It would be highly desirable to develop a theory of the dipole/exchange modes of such entities. We shall address such questions in future studies.

The outline of this paper is as follows. In Sec. II, we present the theory of the exchange/dipole spin wave modes, and in Sec. III we provide numerical studies of the spin wave dispersion and ferromagnetic resonance response. We also discuss differences between the mode structure and response characteristics of the nanowire, and the well known case of the thin film. In regard to the microwave response, for the case where the sample is made of conducting material, there are very substantial differences between the two cases. Section IV is devoted to concluding remarks.

## II. THEORETICAL DISCUSSION

In this section, we first present the theory of the spin-wave excitations of a long ferromagnetic nanowire with circular cross section, and magnetization parallel to its axis. Then we turn to a description of its response to a spatially uniform microwave field, appropriate to a ferromagnetic resonance experiment. Throughout this section, the magnetization is assumed parallel to the  $z$  axis, which is also parallel to the symmetry axis of the nanowire.

As mentioned in Sec. I, we develop here the theory of the spin waves of the nanowire, with emphasis on the regime where both exchange and dipolar couplings between the spins are comparable in magnitude. However, before we turn to this general analysis, it will be useful for what follows to have in hand a summary of the theory of dipolar spin waves, in the absence of exchange. This will serve also to introduce notation used throughout the paper.

In the linearized version of spin wave theory, when a mode is excited the magnetization of the sample is given by

$$\mathbf{M}(\mathbf{r}, t) = \hat{z}M_S + \hat{x}m_x(\mathbf{r})\exp(-i\Omega t) + \hat{y}m_y(\mathbf{r})\exp(-i\Omega t), \quad (1)$$

where for any nanowire of uniform cross section,  $m_\alpha(x, y, z) = m_\alpha(x, y)\exp(ikz)$ , where  $k$  is the wave vector of the mode, in the direction parallel to the axis of symmetry. The precession of the magnetization generates a magnetic field of dipolar origin, with frequency  $\Omega$ . We call this  $\mathbf{h}^d$ . The dependence of the dipolar field on  $z$  is the same as that given above. In the absence of exchange, the components of the dipolar field and those of the transverse magnetization are linked by the constitutive relations, suppressing explicit reference to time dependence for brevity,

$$m_x(x, y) = \chi_1(\Omega)h_x^d(x, y) + i\chi_2(\Omega)h_y^d(x, y) \quad (2a)$$

and

$$m_y(x, y) = \chi_1(\Omega)h_y^d(x, y) - i\chi_2(\Omega)h_x^d(x, y), \quad (2b)$$

where for a ferromagnet,  $\chi_1(\Omega) = \Omega_H\Omega_M/(\Omega_H^2 - \Omega^2)$  and  $\chi_2(\Omega) = \Omega\Omega_H/(\Omega_H^2 - \Omega^2)$ . If  $\gamma$  is the gyromagnetic ratio and  $H_0$  an applied dc magnetic field parallel to the magnetization, we have introduced  $\Omega_H = \gamma H_0$  and  $\Omega_M = \gamma M_S$ . Within the magnetostatic approximation, the dipole field may be expressed as the gradient of the magnetic potential

$$\mathbf{h}^d(\mathbf{r}) = -\nabla\Phi_M(\mathbf{r}), \quad (3)$$

where again  $\Phi_M(\mathbf{r}) = \Phi_M(x, y)\exp(ikz)$ . Inside the nanowire, the induction  $\mathbf{b} = \mathbf{h}^d + 4\pi\mathbf{m}$ , while outside  $\mathbf{b} = \mathbf{h}^d$ . The magnetostatic theory of spin waves, with exchange ignored, follows by exploring the solutions of  $\nabla \cdot \mathbf{b} = 0$  everywhere, with the solution subject to the condition that the normal (radial, in this case) component of  $\mathbf{b}$  be continuous across the surface, while tangential (azimuthal,  $z$ ) components of  $\mathbf{h}^d$  are continuous. Inside the cylinder, the magnetic potential satisfies Walker's equation<sup>2</sup>

$$\left[1 + 4\pi\chi_1(\Omega)\right]\left(\frac{\partial^2}{\partial x^2} + \frac{\partial^2}{\partial y^2}\right)\Phi_M(x, y) - k^2\Phi_M(x, y) = 0 \quad (4)$$

while outside, one sets  $\chi_1(\Omega)$  to zero. We let  $\mu_1(\Omega) = 1 + 4\pi\chi_1(\Omega)$  and  $\mu_2(\Omega) = 4\pi\chi_2(\Omega)$  in what follows.

For the problem of interest, we use cylindrical coordinates, and seek solutions for which the magnetic potential has the form  $\Phi_M(\rho, \phi) = f_m(\rho)\exp(im\phi)$ . We shall focus our attention here on the frequency regime where  $\mu_1(\Omega)$  is positive. Then inside the nanowire, one has  $f_m^<(\rho) = AI_m[k\rho/\mu_1(\Omega)^{1/2}]$  while outside one has  $f_m^>(\rho) = BK_m(k\rho)$ , where  $I_m$  and  $K_m$  are the modified Bessel functions.

Application of the boundary conditions described above at the surface of the nanowire, where  $\rho = R$ , leads one to the implicit dispersion relation from which the frequency of the magnetostatic modes are found:

$$\mu_1^{1/2}\left\{\frac{I'_m(kR/\mu_1^{1/2})}{I_m(kR/\mu_1^{1/2})}\right\} - \frac{m\mu_2}{kR} = \frac{K'_m(kR)}{K_m(kR)}. \quad (5)$$

In this expression,  $I'_m$  and  $K'_m$  are derivatives of the modified Bessel functions with respect to their argument.

For what follows, our interest will reside in the behavior of the magnetostatic modes at very long wavelengths, in the regime  $kR \ll 1$ . Through use of the appropriate series expansions for the modified Bessel functions in Eq. (5), one may obtain analytic expressions for the frequencies of the various modes. We denote, for a given choice of the wave vector  $k$  and the azimuthal quantum number  $m$  the frequency of the mode by  $\Omega_m(k)$ . One then has

$$|\Omega_1(k)| = -\Omega_1(k) = H_0 + 2\pi M_S - \pi M_S(kR)^2 \ln\left(\frac{2}{kR}\right) + \dots, \quad (6a)$$

while for  $m > 1$

$$|\Omega_m(k)| = -\omega_m(k) = H_0 + 2\pi M_S - \frac{\pi M_S}{(m^2 - 1)}(kR)^2 + \dots. \quad (6b)$$

These results require some comment. First of all, when the azimuthal quantum number is positive, as assumed in deriving Eqs. (6), the frequencies are all negative, as one sees from these results. These modes all describe a circulation of energy in the counterclockwise sense around the cylinder, as one looks down the magnetization. If we had chosen the

azimuthal quantum number negative, the frequencies would have all been positive; the frequency is an odd function of  $m$  as one can appreciate from the structure of Eq. (5). Thus the entire spectrum of magnetostatic modes describes a circulation of energy around the magnetization, with the counter-clockwise sense.

As the wave vector  $k \rightarrow 0$ , all the magnetostatic modes approach the frequency  $H_0 + 2\pi M_S$ . This is the ferromagnetic resonance frequency of the cylindrical nanowire. When this uniform ferromagnetic resonance mode is excited, the transverse magnetization engages in circular precession about the static magnetization, and generates an internal, spatially uniform demagnetizing field of strength  $2\pi M_S$  as it does so. As we move off to finite wave vectors, the magnetic dipole interactions produce a negative dispersion initially, so the frequency of the spin wave modes drops below that of the ferromagnetic resonance mode. We will see below that when exchange is added, a positive contribution to the dispersion is produced for many of the modes, so the minimum frequency can lie away from  $k=0$ .

A complete description of the spin-wave modes of the cylinder requires us to include the influence of exchange. We now turn to this question.

### A. Spin wave dispersion in the presence of exchange

In the macroscopic description of the spin excitations, the magnetic field  $\mathbf{h}^d$  inside and outside the cylinder is still described through introduction of a magnetic potential as in Eq. (3), and we still require that  $\nabla \cdot \mathbf{b} = 0$  everywhere, just as before. However, we no longer can utilize Eqs. (2) to relate the transverse magnetization components to the dipolar field. We must resort to the Landau-Lifshitz equation of motion instead, and in this one incorporates the exchange field a given spin experiences from its neighbors. This may be done by replacing the spatially uniform dc magnetic field by the effective field  $\hat{z}(H_0 - D\nabla^2)$ , where  $D$  is the exchange stiffness. This leads us to the following relations:

$$i\Omega m_x = (H_0 - D\nabla^2)m_y + M_S \frac{\partial \Phi_M}{\partial y}, \quad (7a)$$

$$-i\Omega m_y = (H_0 - D\nabla^2)m_x - M_S \frac{\partial \Phi_M}{\partial x} \quad (7b)$$

while inside the material, the  $\nabla \cdot \mathbf{b} = 0$  condition becomes

$$\nabla^2 \Phi_M - 4\pi \left( \frac{\partial m_x}{\partial x} + \frac{\partial m_y}{\partial y} \right) = 0. \quad (7c)$$

Outside the material, the magnetic potential satisfies Laplace's equation. Of course, when the exchange stiffness is set to zero, Eqs. (7a) and (7b) produce results equivalent to those in Eq. (2).

Some manipulation is required to cast Eqs. (7) into a form where one may extract the structure of the solution, for the geometry of present interest. We first rewrite the equations, to express them in terms of the right and left circularly po-

larized variables  $m_{+,-} = m_x \pm im_y$ , and similarly for the dipole field components. Then Eqs. (7) are replaced by

$$(\Omega + H_0 - D\nabla^2)m_+ = M_S h_+^d, \quad (8a)$$

$$(\Omega - H_0 + D\nabla^2)m_- = -M_S h_-^d, \quad (8b)$$

and

$$\nabla^2 \Phi_M - 2\pi \left[ \left( \frac{\partial}{\partial x} - i \frac{\partial}{\partial y} \right) m_+ + \left( \frac{\partial}{\partial x} + i \frac{\partial}{\partial y} \right) m_- \right] = 0. \quad (8c)$$

In what follows, we shall utilize the identities

$$\left( \frac{\partial}{\partial x} - i \frac{\partial}{\partial y} \right) h_+^d = \left( \frac{\partial}{\partial x} + i \frac{\partial}{\partial y} \right) h_-^d = -\nabla_{\perp}^2 \Phi_M, \quad (9)$$

where  $\nabla_{\perp}^2 = (\partial^2/\partial x^2 + \partial^2/\partial y^2)$ . We next introduce the auxiliary quantities

$$f_+ = \left( \frac{\partial}{\partial x} - i \frac{\partial}{\partial y} \right) m_+ \quad (10a)$$

and

$$f_- = \left( \frac{\partial}{\partial x} + i \frac{\partial}{\partial y} \right) m_-. \quad (10b)$$

Then one may rewrite Eq. (8c) to read

$$f_+ + f_- = \frac{1}{2\pi} \nabla^2 \Phi_M, \quad (11)$$

while Eqs. (8a) and (8b) may be rearranged to state

$$\Omega(f_+ + f_-) + (H_0 - D\nabla^2)(f_+ - f_-) = 0 \quad (12a)$$

and

$$\Omega(f_+ - f_-) + (H_0 - D\nabla^2)(f_+ + f_-) = -2M_S \nabla_{\perp}^2 \Phi_M. \quad (12b)$$

Upon combining Eq. (12a) with Eq. (12b), one may relate  $(f_+ - f_-)$  to the potential  $\Phi_M$ . When this statement and Eq. (11) are substituted into Eq. (12a), we obtain a homogeneous equation that must be satisfied by the magnetic potential

$$[(D\nabla^2 - H_0)(D\nabla^2 - B_0)] \nabla^2 \Phi_M + 4\pi M_S (D\nabla^2 - H_0) \frac{\partial^2}{\partial z^2} \Phi_M = 0. \quad (13)$$

In Eq. (13), we introduce  $B_0 = H_0 + 4\pi M_S$ .

One finds that Eq. (13) admits solutions of the form

$$\Phi_M(\rho, \phi, z) = J_m(\kappa\rho) \exp(im\phi + ikz). \quad (14)$$

If Eq. (14) is inserted into Eq. (13), and one notes that

$$\left[ \frac{1}{\rho} \frac{d}{d\rho} \rho \frac{d}{d\rho} + \left( \kappa^2 - \frac{m^2}{\rho^2} \right) \right] J_m(\kappa\rho) = 0, \quad (15)$$

then for Eq. (14) to be a solution of Eq. (13),  $\kappa$  must be a root of

$$D^2(\kappa^2 + k^2)^3 + D(H_0 + B_0)(\kappa^2 + k^2)^2 + (H_0 B_0 - \Omega^2 - 4\pi M_S D k^2)(\kappa^2 + k^2) - 4\pi M_S H_0 k^2 = 0. \quad (16)$$

Since Eq. (16) is a cubic equation in  $\kappa^2$ , for each choice of  $m$  and  $k$ , there are three linearly independent solutions of Eq. (14). Thus, we write the magnetic potential inside the material in the form

$$\Phi_M(\rho, \phi, z) = \sum_{i=1}^3 A_i J_m(\kappa_i \rho) \exp(im\phi + ikz). \quad (17)$$

Outside the cylinder, the magnetic potential satisfies Laplace's equation precisely as in the magnetostatic theory, so once again for  $\rho > R$  we have

$$\Phi_M(\rho, \phi, z) = B K_m(k\rho) \exp(im\phi + ikz). \quad (18)$$

To find the dispersion relation of the spin waves, through application of the boundary conditions, we shall obtain four homogeneous equations for the four coefficients in the magnetic potential, as displayed in Eqs. (17) and (18). Two of the boundary conditions are continuity of the magnetic potential (this assures continuity of tangential components of  $\mathbf{h}^d$ ) and continuity of  $b_\rho$ . We shall have two other boundary conditions on the transverse components of magnetization, stated below. To apply the boundary conditions, within the material we need explicit expressions for the radial and azimuthal components of the transverse magnetization. To obtain these, we expand these components in a Bessel function series and use Eqs. (8a) and (8b), noting Eq. (15). The following operator identities are useful:

$$\frac{\partial}{\partial x} + i \frac{\partial}{\partial y} = e^{i\phi} \left( \frac{\partial}{\partial \rho} - \frac{i}{\rho} \frac{\partial}{\partial \phi} \right) \quad (19a)$$

and

$$\frac{\partial}{\partial x} - i \frac{\partial}{\partial y} = e^{-i\phi} \left( \frac{\partial}{\partial \rho} + \frac{i}{\rho} \frac{\partial}{\partial \phi} \right). \quad (19b)$$

One finds the following expressions for the two components of magnetization:

$$m_+(\rho, \phi, z) = -\frac{M_S}{4\pi} \left( \sum_{i=1}^3 \frac{\kappa_i A_i J_{m+1}(\kappa_i \rho)}{[D(\kappa_i^2 + k^2) + H_0 + \Omega]} \right) \times \exp[i(m+1)\phi + ikz] \quad (20a)$$

and

$$m_-(\rho, \phi, z) = -\frac{M_S}{4\pi} \left( \sum_{i=1}^3 \frac{\kappa_i A_i J_{m-1}(\kappa_i \rho)}{[D(\kappa_i^2 + k^2) + H_0 - \Omega]} \right) \times \exp[i(m-1)\phi + ikz] \quad (20b)$$

The two boundary conditions which supplement those of magnetostatics refer to the behavior of the magnetization at the cylinder surface. If one considers an idealized Heisenberg ferromagnet, and examines the behavior of the spin wave eigenfunction at the sample surface, in the long wave length limit, it is well known that one must require that the normal derivative of the transverse components of magnetization vanish there. We wish to consider the possibility that surface anisotropy is present on the cylinder surface; its presence influences the boundary condition. We assume that the

surface anisotropy contributes a term to the surface energy of our cylinder in the form  $-K_S(m_\rho/M_S)^2$ , where the units of  $K_S$  is ergs/cm<sup>2</sup>. When  $K_S$  is positive, the normal to the surface is an easy axis, and when it is negative, the normal to the surface is a hard axis. In terms of the standardly defined exchange stiffness used often in the literature on ferromagnetism!, then the boundary conditions for the transverse magnetization become

$$\left( \frac{\partial m_\phi}{\partial \rho} \right)_{\rho=R} = 0, \quad (21a)$$

$$A \left( \frac{\partial m_\rho}{\partial \rho} \right)_{\rho=R} - \left( \frac{2K_S}{M_S} \right) m_\rho|_{\rho=R} = 0. \quad (21b)$$

The exchange stiffness  $D$  in our formulas has units of Ga-cm<sup>2</sup>. It is proportional to  $A$ , and in fact  $D = 2A/\mu_B M_S$ , where  $\mu_B$  is the Bohr magneton.

This completes our discussion of the formalism for the description of the exchange/dipole spin wave excitations of a ferromagnetic nanowire of cylindrical cross section. We describe numerical calculations based on this description in Sec. III. We turn next to the theory of the microwave response of a conducting ferromagnetic nanowire, before we present the numerical results.

### B. The microwave response of an isolated ferromagnetic nanowire

In this section, we present the theory of the microwave response of the nanowire considered above, with exchange and the presence of surface anisotropy included. The geometry is the same as that considered in the previous section. We have a nanowire, whose saturation magnetization is directed parallel to its symmetry axis. It is the case as well that the samples employed in the experiments which motivated this study are metallic in nature, so we wish to include the influence of the conductivity of the wire on its response. In essence, the microwave fields to which the wire is exposed create eddy currents which produce a finite skin depth. This influences the spatial profile of the exciting field within the sample, though the discussion presented in Sec. III will show that the influence of the skin depth is much more modest for the cylindrical geometry, compared to the ultrathin film.

In what follows, it is assumed that the microwave magnetic field of interest is spatially uniform far from the wire, and is parallel to the  $x$  direction. All quantities will be assumed independent of  $z$  in what follows. Such a microwave field excites the magnetization of the sample, of course, so the field is inhomogeneous near the wire, but always in the plane, and independent of  $z$ . By Faraday's Law, the time varying magnetic field generates an electric field, parallel to  $z$ . It is this electric field which is responsible for the eddy currents in the conducting material that lead to the skin effect.

We may describe these fields by introducing the vector potential

$$\mathbf{A}(x, y; t) = \hat{z} A(x, y) \exp(-i\Omega t). \quad (22)$$

Then, upon dropping explicit reference to the time dependence of various quantities once again, the electric field is given by

$$\mathbf{e}(x,y) = i \frac{\Omega}{c} \hat{z} A(x,y). \quad (23)$$

The magnetic field  $\mathbf{h}$  is linked to the electric field via

$$\nabla \times \mathbf{h} = \frac{4\pi}{c} \mathbf{j} = \frac{4\pi\sigma}{c} \hat{z} e = \frac{2i}{\delta_0^2} \hat{z} A, \quad (24)$$

where  $\sigma$  is the conductivity of the material. We have introduced the classical skin depth  $\delta_0 = c/(2\pi\sigma\Omega)^{1/2}$ . In Eq. (24), we ignore the displacement current term in the Maxwell equation. If this were to be included, its influence can be absorbed into a correction to the formula for the skin depth. The correction is of no quantitative importance at microwave frequencies, for typical metals.

The magnetic induction  $\mathbf{b} = \nabla \times \mathbf{A}$ , and of course  $\mathbf{h} = \mathbf{b} - 4\pi\mathbf{m}$ . When these statements are combined with Eq. (24), and it is noted that all quantities are independent of  $z$ , we find

$$\left[ \nabla_{\perp}^2 + \frac{2i}{\delta_0^2} \right] A = 4\pi \left[ \frac{\partial m_x}{\partial y} - \frac{\partial m_y}{\partial x} \right], \quad (25)$$

where the operator  $\nabla_{\perp}^2$  is introduced just after Eq. (9). Additional relations between the magnetization and the vector potential follow from the Landau Lifshitz equations. We use analogs of Eq. (7), where now the field  $\mathbf{h} = \nabla \times \mathbf{A} - 4\pi\mathbf{m}$ , rather than  $-\nabla\phi_M$  as earlier, and we also add to the right hand side the damping term  $(G/M_S^2)(\mathbf{M} \times d\mathbf{M}/dt)$ , with  $G$  the Gilbert damping factor. We then find, with all quantities once again expressed in magnetic field units

$$i\Omega m_x = [\tilde{B}_0 - D\nabla_{\perp}^2] m_y + M_S \frac{\partial A}{\partial x}. \quad (26a)$$

and

$$i\Omega m_y = -[\tilde{B}_0 - D\nabla_{\perp}^2] m_x + M_S \frac{\partial A}{\partial y}. \quad (26b)$$

We have introduced  $\tilde{B}_0 = H_0 + 4\pi M_S + ig\Omega$ , where  $g = G/\gamma M_S$ . After a bit of manipulation, from Eq. (26), we may obtain the statement that

$$\begin{aligned} & [(\tilde{B}_0 - D\nabla_{\perp}^2)^2 - \Omega^2] \left( \frac{\partial m_x}{\partial y} - \frac{\partial m_y}{\partial x} \right) - M_S (\tilde{B}_0 - D\nabla_{\perp}^2) \nabla_{\perp}^2 A \\ & = 0, \end{aligned} \quad (27)$$

which when combined with Eq. (25) provides us with two equations that link the vector potential with the quantity

$$F(x,y) = \frac{\partial m_x}{\partial y} - \frac{\partial m_y}{\partial x}. \quad (28)$$

For constructing explicit expressions for the components of transverse magnetization, it is useful to note the relation

$$i\Omega \left( \frac{\partial m_x}{\partial x} + \frac{\partial m_y}{\partial y} \right) = [\tilde{B}_0 - D\nabla_{\perp}^2] F + M_S \nabla_{\perp}^2 A. \quad (29)$$

The combination of Eqs. (25) and (27) admit solutions of the form

$$A = a J_m(\kappa\rho) \exp(im\phi) \quad (30a)$$

and

$$F = b J_m(\kappa\rho) \exp(im\phi). \quad (30b)$$

When these forms are substituted into the two equations, we find that  $\kappa$  satisfies

$$\begin{aligned} & D^2 \kappa^6 + \left[ 2(\tilde{H}_0 + 2\pi M_S) D - \frac{2iD^2}{\delta_0^2} \right] \kappa^4 + \left[ \tilde{B}_0 \tilde{H}_0 - \frac{4iD\tilde{B}_0}{\delta_0^2} \right. \\ & \left. - \Omega^2 \right] \kappa^2 - \frac{2i}{\delta_0^2} [\tilde{B}_0^2 - \Omega^2] = 0. \end{aligned} \quad (31)$$

Here we have  $\tilde{H}_0 = H_0 + ig\Omega$ . Notice in the limit that the skin depth is allowed to become infinite and also when damping is ignored, Eq. (31) reduces to Eq. (13) if there we set  $k$  equal to zero.

There are three independent solutions of Eq. (31) for  $\kappa$ . Thus, the most general solution for the vector potential in the medium, with the azimuthal variation as given in Eq. (30a), is

$$A(\rho, \phi) = \sum_{i=1}^3 a_i J_m(\kappa_i \rho) \exp(im\phi). \quad (32)$$

For the purpose of applying boundary conditions at the surface of the cylinder, we require explicit expressions for the magnetization, and for the components of magnetic field generated by the motion of the magnetization. It is most convenient for these to be expressed in cylindrical components. After some algebra which employs standard Bessel function identities, we find

$$\begin{aligned} m_{\rho}(\rho, \phi) = & i \frac{M_S}{2} \sum_{i=1}^3 a_i \kappa_i \left\{ \frac{J_{m+1}(\kappa_i \rho)}{\tilde{B}_0 + D\kappa_i^2 + \Omega} \right. \\ & \left. + \frac{J_{m-1}(\kappa_i \rho)}{\tilde{B}_0 + D\kappa_i^2 - \Omega} \right\} \exp(im\phi), \end{aligned} \quad (33a)$$

$$\begin{aligned} m_{\phi}(\rho, \phi) = & \frac{M_S}{2} \sum_{i=1}^3 a_i \kappa_i \left\{ \frac{J_{m+1}(\kappa_i \rho)}{\tilde{B}_0 + D\kappa_i^2 + \Omega} \right. \\ & \left. - \frac{J_{m-1}(\kappa_i \rho)}{\tilde{B}_0 + D\kappa_i^2 - \Omega} \right\} \exp(im\phi), \end{aligned} \quad (33b)$$

$$b_{\rho}(\rho, \phi) = \frac{im}{\rho} \sum_{i=1}^3 a_i J_m(\kappa_i \rho) \exp(im\phi), \quad (34a)$$

$$b_\phi(\rho, \phi) = -\frac{1}{2} \sum_{i=1}^3 a_i \kappa_i \{J_{m+1}(\kappa_i \rho) - J_{m-1}(\kappa_i \rho)\} \exp(im\phi), \quad (35a)$$

and the electric field is given in Eq. (23). We now need to match the interior solutions just described to the fields outside the cylindrical nanowire. It is a simple matter to generate expressions for the magnetic and electric field in the vacuum outside, following a simplified version of the method just given. One may generate an expression for the vector potential in spherical coordinates through the wave equation in vacuum, then use this to find the components of the various fields. We do this assuming the limit  $\Omega R/c \ll 1$  applies for the nanostructures of interest; in the near vicinity of the nanowire, the incident microwave field is viewed as spatially uniform, with magnitude  $h_0$ , and also parallel to the  $x$  axis. We have outside the cylinder the incident field, supplemented by that generated by the motion of the magnetization in the nanowire; the latter will vary with the azimuthal angle as  $\exp(\pm i\phi)$  in the limit the incident field is approximated as spatially uniform outside the wire. Then for the fields outside we find

$$h_\rho^>(\rho, \phi) = h_0 \cos(\phi) + i \frac{b_+}{\rho^2} \exp(i\phi) + i \frac{b_-}{\rho^2} \exp(-i\phi), \quad (36a)$$

$$h_\phi^>(\rho, \phi) = h_0 \sin(\phi) + \frac{b_+}{\rho^2} \exp(i\phi) + \frac{b_-}{\rho^2} \exp(-i\phi) \quad (36b)$$

and for the magnitude of the electric field, we have

$$e(\rho, \phi) = i \frac{\Omega}{c} \left\{ h_0 \rho \sin(\phi) + \frac{b_+}{\rho} \exp(i\phi) + \frac{b_-}{\rho} \exp(-i\phi) \right\}. \quad (36c)$$

Our next task is to apply the boundary conditions. The solutions inside the medium are formed by superimposing the  $m = +1$  and  $m = -1$  forms given above. Thus, we have six unknown amplitudes associated with the solution in the interior of the wire, and as one sees from Eq. (36) there are two more associated with the fields outside, for a total of 8. The boundary conditions on the fields are of course that the magnitude of the (tangential) electric field be conserved across the boundary, along with continuity of  $b_\rho$  and  $h_\phi$ . The conservation of  $b_\rho$  and tangential electric field yield identical constraints, so from the field conservation conditions, we have two independent statements. We also apply the boundary conditions on the magnetization given in Eq. (21). When these four statements are broken down, with components proportional to and components proportional to  $\exp(+i\phi)$  separated, we obtain eight inhomogeneous equations from which the unknown amplitudes may be expressed in terms of  $h_0$ . We will not quote the explicit form of these statements here, since they may be derived readily from the information given above. As remarked earlier, in Sec. III, we present a series of numerical studies based on the formalism just given.

### III. NUMERICAL STUDIES OF THE EXCHANGE/DIPOLE SPIN WAVE MODES AND THE MICROWAVE RESPONSE OF FERROMAGNETIC NANOWIRES

#### A. The nature of the spin wave modes

First, we begin with some general remarks. An interesting question is the initial behavior of the spin wave dispersion curves in the limit of small wave vector  $k$ . If initially, there is downward curvature, then the minimum frequency of a given branch will be at a finite, nonzero wave vector, since we can expect exchange to dominate at large values of the wave vector. Conversely, if the initial curvature is positive, then we may expect the minimum to reside at zero wave vector.

To examine this behavior, as one sees from Eqs. (6), we need to consider the case  $m = 1$  separately from the case where  $m > 1$ . As we have seen from Sec. II B, the zero wave vector modes with  $m = 1$  are the modes excited by a spatially uniform microwave field.

We may expect exchange to add a term to the dispersion relation proportional to  $Dk^2$ , of course. If we then examine Eq. (6a), we see that by virtue of the logarithmic term, in the long wavelength limit, the negative dispersion from the dipolar contribution will always dominate that from exchange. However, since the prefactor of the logarithm is proportional to  $(kR)^2$ , for nanowires of small radii the dipolar term will assert itself only at very small values of the wave vector. One sees easily that the dipolar term will dominate the long wavelength form of the dispersion relation only when  $k < (2/R) \exp(-D/\pi M_S R^2)$ . Thus, while for  $m = 1$ , we expect the minimum frequency of the magnetostatic mode to always lie away from zero wave vector, but in numerical calculations for nanowires of small radii, the initial negative dispersion will be a subtle feature. At larger values of the radius, we will see the negative dispersion clearly.

For the modes with  $m > 2$ , from Eq. (6b), we see that the dipolar contributions to the dispersion provide negative dispersion in the form of a term quadratic in the wave vector, with prefactor scaling also as  $R^2$ . Since an exchange contribution  $Dk^2$  is independent of radius, we expect to see positive dispersion in these modes for nanowires of small radii, and then for nanowires of larger radii, we will realize negative dispersion initially, with the minimum frequency of a given branch shifted away from zero wave vector.

One may cast the discussion of the spin-wave dispersion relation in terms of two-dimensionless parameters  $h = H_0/4\pi M_S$  and  $p = l/R$ , and, where  $l = (D/4\pi M_S)^{1/2}$  is an exchange length. For Ni, the exchange length is roughly 58 Å, while for Fe it is 35 Å. In what follows, we use the reduced frequency  $\omega = \Omega/4\pi M_S$ , and the frequencies will be plotted against the logarithm of  $kR$ .

In Fig. 1(a), for  $m = 1$  and for  $h = 0.19$  (this corresponds to an applied dc field of 4 kG for Fe), we show the spin wave dispersion for the case where  $p = 2$ . Within the range of frequencies displayed, there is one mode only, which in the limit of zero wave vector approaches the FMR frequency, which in our dimensionless units has the frequency  $h + 1/2$ . The negative dispersion at small wave vectors discussed above does not show, on the scale of this plot. Clearly, by the time the parameter  $kR$  approaches unity, the excitation en-

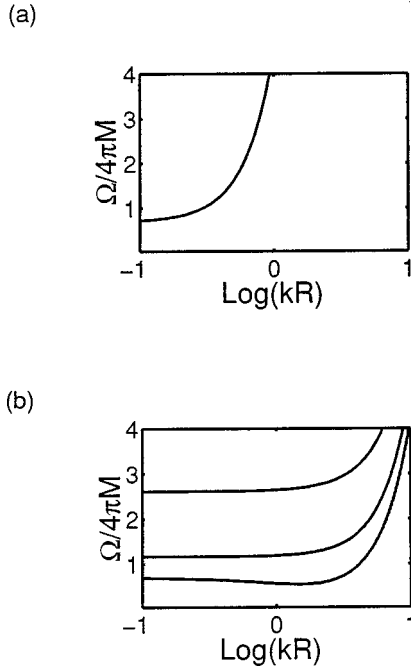


FIG. 1. For the case where  $m=1$ , and for  $h=H_0/4\pi M_S=0.19$ , we show the spin-wave frequencies plotted as a function of  $\ln(kR)$  for (a)  $p=2$  and (b)  $p=0.2$ , where  $p$  is the ratio of the exchange length defined in the text and the radius of the nanowire.

ergy of the spin wave is dominated by exchange for nanowires of such small radius. In Fig. 1(b), for the same applied magnetic field, and again for  $m=1$ , we show dispersion curves for nanowires of much larger radius, where  $p=0.2$ . We now see several standing wave exchange branches, whose frequency at zero wave vector is above that of the FMR mode. Also, at these larger radii, for the mode that approaches the FMR frequency at long wavelengths, the negative dispersion at small wave vectors is now evident in the plot.

We find very interesting behavior at much larger radii, as illustrated in Fig. 2. These calculations again are for  $m=1$  and  $h=0.19$ , but now we have  $p=0.05$ . In the case of Ni, this would describe a nanowire whose radius is a bit under 1200 Å. We now have a larger number of more closely spaced exchange branches, as expected, but now notice that there are two exchange modes which lie below the ferromagnetic resonance frequency, in the limit of zero wave vector. The magnetostatic mode that approaches the FMR frequency as  $k \rightarrow 0$  shows large negative dispersion at small wave vectors, until exchange takes over, and in fact we see that the magnetostatic mode hybridizes with the low frequency exchange modes, as the wave vector increases.

This set of dispersion curves, and the comparison between Fig. 2 and Fig. 1(b) requires some comment. Let us consider the basic solutions we encounter in the limit the wave vector  $k$  is zero. If we think of infinitely extended ferromagnetic matter for the moment, then we shall have spin waves that propagate within the  $xy$  plane, whose frequency is given by the well known expression  $\Omega(\kappa)=[(H_0+D\kappa^2)(H_0+4\pi M_S+D\kappa^2)]^{1/2}$ , where we denote them in plane wave vector as  $\kappa$ . When such a wave is confined to within a cyl-

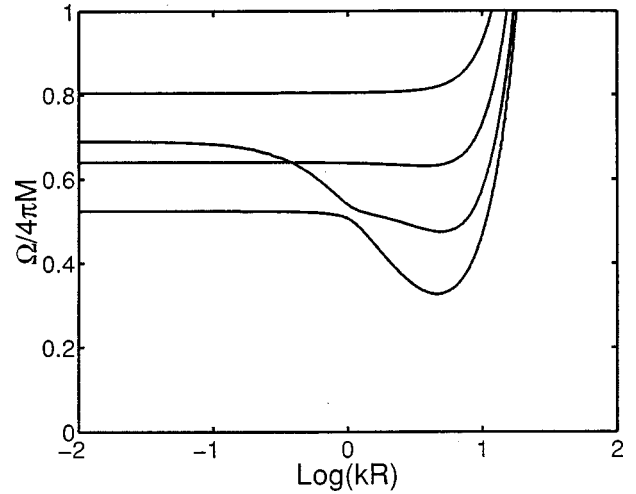


FIG. 2. For  $m=1$ ,  $h=0.19$ , and  $p=0.05$ , we show the spin-wave frequencies of the nanowire plotted as a function of  $\ln(kR)$ .

inder of finite radius  $R$ ,  $\kappa$  will obtain quantized values in the range of  $\kappa=\kappa_n=n\pi/R$ , where the lowest standing mode has  $n=1$ . There is in addition a uniform mode of the cylinder, wherein the magnetization engages in perfectly circularly polarized precession at the FMR frequency  $H_0+2\pi M_S$ , which, it will be noted, lies higher in frequency than  $\Omega(\kappa=0)$ . In the cylinder, in the presence of the boundaries, the boundary conditions mix the uniform FMR mode with the standing wave exchange modes, so to speak. Now if the radius of the nanowire is so small that  $\Omega(\kappa=\pi/R)$  lies above the FMR frequency, we have a situation where one of the modes, which we have referred to above as the magnetostatic mode, approaches the FMR frequency as  $k \rightarrow 0$ , while all the standing wave exchange modes lie above this frequency. This is the case for the example given in Fig. 1(b). Now as the radius of the cylinder is increased, one or more of the modes of frequency  $\Omega(\kappa_n)$  will drop below the FMR frequency. In the limit  $k \rightarrow 0$ , we thus have standing wave exchange modes which lie below the FMR frequency. This is the case for the example in Fig. 2. The magnetostatic mode, which approaches the FMR frequency in this limit, exhibits negative dispersion at small wave vectors as expected from Eq. (6a), and the boundary conditions lead to the hybridization with the exchange modes evident in Fig. 2.

The situation just described is very different than realized in the much studied case of the thin film magnetized parallel to its surfaces. We still have the in plane standing wave exchange modes, with the frequency  $\Omega(\kappa)$  just as above, but now the uniform mode that mixes with these is elliptically polarized, with frequency  $[H_0(H_0+4\pi M_S)]^{1/2} \equiv \Omega(0)$ . The standing wave spin waves always lie above the ferromagnetic resonance frequency.

These comments have implications for ferromagnetic resonance studies for nanowires, where the response of the sample is probed at fixed frequency, and the external dc magnetic field is swept. In the thin film, the standing wave exchange resonances are always found at resonance fields below the main FMR resonance field (provided, of course, there are no perturbations at the boundary so large as to



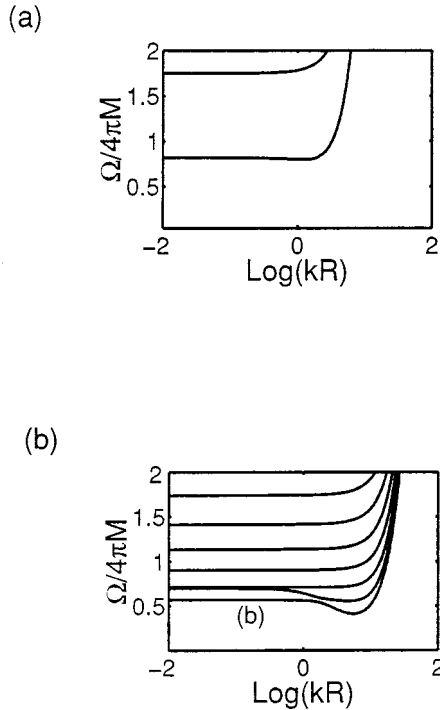


FIG. 3. For  $m=2$ ,  $h=0.19$  and (a)  $p=0.2$  and (b)  $p=0.05$ , we show the spin wave frequencies plotted as a function of  $\ln(kR)$ .

produce spin waves tightly bound to the surface). It will be the case as well that in nanowires of small radius, the standing wave resonances will lie lower in field than the main FMR line. However as the radius of the nanowire is increased, one reaches a point where one may find standing wave resonances of the structure at fields above the FMR field; such lines will be produced by the exchange modes that have dropped below the FMR frequency.

In Fig. 3 and in Fig. 4, we show dispersion curves for modes with  $m=2$  and  $m=3$ , respectively. One sees that for the samples of small diameter, the dispersion is positive at long wavelengths, whereas one sees negative dispersion at larger radii, as expected from the discussion above.

### B. The microwave response of conducting ferromagnetic nanowires

We next turn to studies of the microwave response of ferromagnetic nanowires, utilizing the formalism given in Sec. II B. All computations below use parameters appropriate to Ni at room temperature, with the experiments of Ref. 1 in mind. We take  $M_S=480$  G, the  $g$  factor to be 2.15, the spin-wave exchange stiffness as  $D=2 \times 10^{-9}$  G-cm<sup>2</sup> and for the purposes of including the influence of the skin depth on the response, the electrical resistivity is 7 mΩ cm. This gives a classical skin depth in the range of a micron at 10 GHz, which is very much larger than the radii of the nanowires considered here.

For the purposes of calculating the FMR spectra, we consider a quantity  $\Gamma$  defined as follows. As we have seen in Sec. II B, the precessing magnetization of the wire creates a strong magnetic field outside the wire, which falls off in-

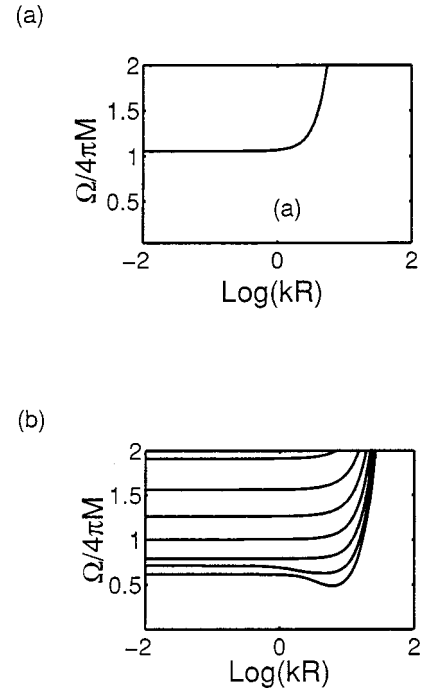


FIG. 4. For  $m=3$ ,  $h=0.19$ , and (a)  $p=0.2$  and (b)  $p=0.05$ , we show the spin wave frequencies plotted as a function of  $\ln(kR)$ .

versely with the square of the distance from the axis of symmetry, as we see from Eqs. (36a) and (36b). The coupling of the nanowire to a detector will scale as the square of the strength of this field. We define  $\Gamma$  to be  $\Gamma = \langle (h_\rho)^2 + (h_\phi)^2 \rangle_{\rho=R^+} / h_0^2$ , where the angular brackets denote an average over the circumference of the wire.

Before we present our results, we comment on the role of the spin depth in the present analysis. Our point is that it differs qualitatively for nanowires from the case of the thin film. First of all, in a conducting magnetic medium, the skin depth is influenced not only by the conductivity of the material, but by its magnetization as well. To good approximation,<sup>9</sup> in place of the classical skin depth  $\delta_0 = c / (2\pi\omega\sigma)^{1/2}$ , penetration of microwave fields is controlled by  $\delta_M = c / (2\pi\omega\sigma\mu_V)^{1/2}$ , where  $\mu_V = (\mu_1^2 - \mu_2^2) / \mu_1$  is the Voigt susceptibility. Here  $\mu_1 = 1 + 4\pi\chi_1$ , and  $\mu_2 = 4\pi\chi_2$ , with  $\chi_1$  and  $\chi_2$  the dynamic susceptibilities defined in Eq. (2). For the picture used here in Sec. II A, one has  $\mu_V = (B_0^2 - \Omega^2) / (H_0 B_0 - \Omega^2)$ .

Now if we wish to consider the ferromagnetic resonance response of thin films, note that their resonance frequency is  $(H_0 B_0)^{1/2}$ . At precisely this frequency, the Voigt susceptibility diverges, if we examine the simple expression above. A consequence is the skin depth collapses to zero. Of course, dissipative effects not included in the simple expression just given limit the divergence, but it is the case that the skin depth collapses to a small value, as one scans through resonance. In a high quality ferromagnetic metal such as Fe, the effective skin depth on resonance can be as small as 500 Å, in the 10 GHz frequency range. The very strong frequency dependence of the skin depth as one scans through resonance means it is essential to include its role, in the discussion of microwave response of thin, conducting ferromagnetic films.

In Ref. 9 and earlier references cited therein, one sees strong influences of the frequency dependence of the skin depth, including the “window” near  $B_0$  where the skin depth becomes very large.

In the ferromagnetic nanowires, we are concerned with much higher frequencies, near  $H_0 + 2\pi M_S$ , where there is no particular resonance or strong frequency dependence in the Voigt susceptibility. The penetration depth of the fields differs only nominally for that expected in the absence of the magnetic response. Thus, for nanowires with radius small compared to the classical skin depth, their finite, metallic conductivity has at most a modest influence on their response.

Further comments along these lines are of interest. To return to the case of the thin metallic film, if the film has thickness small compared to the renormalized skin depth on resonance, a situation encountered commonly in the study of the FMR of ultrathin films, one might suppose that within the film, the microwave exciting field is uniform to excellent approximation. This is not the case, if the film is illuminated by a microwave field incident from one side. In such a case, it is an elementary matter to see that within the film, if its thickness  $d$  is thin compared to the skin depth, and also the skin depth is thin compared to a vacuum wavelength, the spatial variation  $h(z)$  of the microwave magnetic field within the films is well approximated by, with  $k_0 = \Omega/c$ ,

$$h(z) = 2h_0 \frac{(1 - z/d) + k_0 \delta_M^2 / 2d}{1 + k_0 \delta_M^2 / d}. \quad (37)$$

Thus, even if the film is very thin compared to the skin depth, the field drops linearly from a value very close to  $2h_0$  at the surface exposed the microwaves, to  $h_0 k_0 \delta_M^2 / d$  at the back surface; the field is highly non uniform within the film, until one reaches thicknesses where  $k_0 \delta_M^2 / d$  is of order unity.

The physical origin of the highly nonuniform magnetic field distribution within a film illuminated from one side, even though its thickness may be small compared to the skin depth, is the poor impedance mismatch between the electromagnetic disturbance within the film, and the transmitted wave on the output surface. The magnetic field thus drops from a value roughly twice that of the incident field on the illuminated surface, to a very small value on the backside of the film. Quite in contrast to this, our conducting nanowire is embedded in a spatially uniform magnetic field, so the profile within the wire is not influenced by such considerations. If the wire radius is small compared to the classical skin depth, the exciting field the wire will be rather uniform in character.

We now present a summary of our studies of the microwave response. The principal conclusions can be summarized quite briefly.

First of all, we have seen that the nanowire admits a rich spectrum of exchange dipole modes in the vicinity of  $k=0$  for the modes with azimuthal quantum number  $m=1$ . We have modes both above and below that of the ferromagnetic resonance frequency, for nanowire diameters in the range of a few hundred Angstroms or more. However, if we assume that the surface anisotropy  $K_S$  vanishes, then the only mode

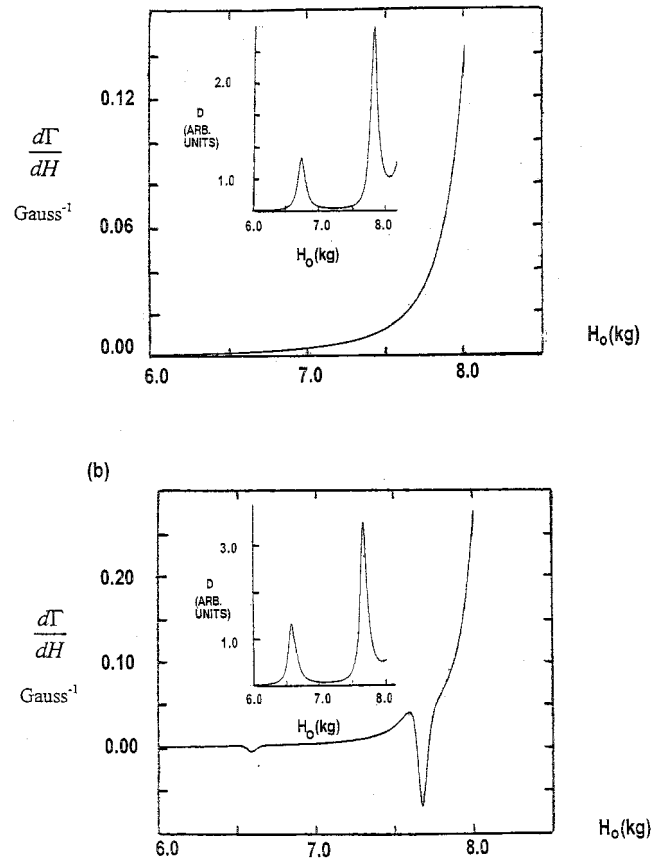


FIG. 5. We illustrate the role of surface anisotropy in activating the standing wave exchange/dipole satellite modes in the ferromagnetic resonance spectrum of the nanowire. The calculations are for a Ni nanowire with radius 1000 Å, and focus on the low field wing of the absorption line. We calculate the derivative with respect to dc field of the ratio  $\Gamma$  defined in the text for (a) the case where the surface anisotropy is zero, and (b) where  $K_S = -0.3$  ergs/cm<sup>2</sup>. The two insets show the inverse of the determinant of the matrix that must be inverted to solve for the magnetization amplitude. The peaks are the positions of the spin wave normal modes. We have used the rather small value  $G = 0.5 \times 10^8$  sec<sup>-1</sup> for the Gilbert damping function, to enhance the satellite features.

we see in the calculated spectrum is the main ferromagnetic resonance mode itself. We have searched even for weak structures from exchange/dipole modes removed from the main FMR mode, to find no evidence of absorption features. It is very much as if there is a hidden theorem we have not been able to prove analytically which forbids all modes other than the FMR mode to be active in microwave excitation when  $K_S = 0$ . It is well known that in the elementary Heisenberg ferromagnet, the standing spin wave resonances are “silent” in the absence of surface spin pinning produced by surface anisotropy, in the limit the microwave exciting field may be viewed as uniform within the film. We were surprised to see the complete absence of all modes except the main FMR mode in our numerical studies of the ideal nanowire, with surface anisotropy absent. In our minds, the existence of a selection rule is not obvious.

We illustrate these remarks in Fig. 5, which shows a por-

tion of the low field wing of the main FMR line of a Ni nanowire 1000 Å in diameter. We have assumed the frequency is 34.4 GHz, as utilized in Ref. 1. Thus, the resonance field is a bit above 8 kG, for our parameters. In Fig. 5(a), we show a region of the low frequency wing, calculated for the case where surface anisotropy is absent. One can perceive no structure whatsoever from exchange/dipole modes. Yet modes exist in this field regime, and illustrated in the inset, where we plot the inverse of the determinant that must be evaluated to find the various field amplitudes in Sec. II B. This determinant has a peak at the field where an exchange dipole mode occurs.

If surface anisotropy is introduced, then the exchange dipole modes ‘‘light up’’ as illustrated in Fig. 5(b). The results displayed here are for the choice  $K_S = -0.3$  ergs-cm<sup>2</sup>, which is a substantial value of the surface anisotropy. Spin pinning to this degree may be realized at the surface if, for example, an oxide layer is present. The principal satellite at the higher field has an intensity of about 1% of that of the main FMR line.

In situations where the nanowire radius is such that an exchange/dipole mode lies quite close in frequency to the FMR mode, the mixing of the two by the boundary conditions can endow the satellite with appreciable integrated strength. This is illustrated in spectra taken by Ebels and Wigen.<sup>1</sup> These authors explore the FMR spectra of Ni nanowires with radius 350, 800, 2700, and 5000 Å. With the exception of the 800 Å sample, a single absorption line is observed. However, for the 800 Å sample, there is a clear doublet. In Fig. 6, we show calculations of the spectrum for three of the sample radii, and indeed we find a doublet very similar in character to that observed. The relative oscillator strength of the two modes is given nicely, when theory is compared to experiment. Not displayed is the calculation for the 5000 Å case, which also shows a single feature as in the data. The calculations in Fig. 6 use  $K_S = -0.85$  ergs/cm<sup>2</sup>, corresponding to a hard axis normal to the nanowire surface. This is again a large value of the surface anisotropy, appropriate to a case where oxide is present on the surface.

#### IV. CONCLUDING REMARKS

We have developed the theory of the exchange/dipole spin wave modes of ferromagnetic nanowires of circular cross section, along with that of their response to spatially uniform microwave exciting fields. We also have presented studies of both the excitations in and the microwave response of samples quite similar to those explored in Ref. 1, and compared the differences between the wire and the well know case of the thin film. We conclude with some additional remarks.

The origin of the linewidth in such samples is of interest. Of course, there is the intrinsic linewidth, described in our phenomenology by the damping term in the Landau Lifshitz equation of motion. In addition, there will be extrinsic mechanisms operative as well. For the case of ultrathin ferromagnetic films, in recent work we have shown<sup>6</sup> that the two magnon mechanism considered many years ago as the source of extrinsic linewidth in the garnets<sup>9</sup> can operate in

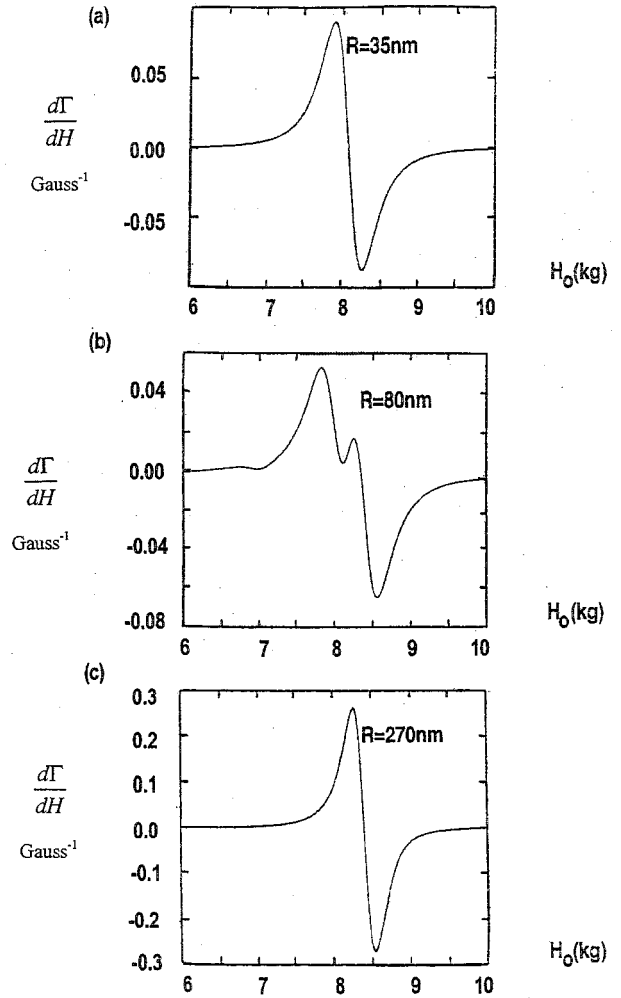


FIG. 6. For three values of the radius of Ni nanowires, (a) 350 Å (b) 800 Å, and (c) 2700 Å, we show calculated ferromagnetic resonance spectra. The calculations employ  $G = 2.5 \times 10^8$  sec<sup>-1</sup> which is a realistic value for Ni, and we have taken  $K_S = -0.85$  ergs/cm<sup>2</sup>.

the ultrathin films as well, by virtue of the fact that in two dimensions, the long ranged dipolar interaction in combination with exchange produces an off center minimum in the spin wave dispersion relation, for a range of propagation directions. This leads to spin wave modes of finite, nonzero wave vector degenerate with the zero wave vector FMR mode. Surface defects (or defects of any other sort) may then scatter energy from the FMR mode to the finite wave vector modes, producing a dephasing contribution to the linewidth. Our predictions seem confirmed by recent experiments.<sup>7</sup> One can inquire if the two magnon mechanism is operative in nanowires as well.

In principle, this mechanism should be operative. First suppose we have a nanowire with undulating surfaces of such character that the wire is still form invariant under rotations about the  $z$  axis. Then from symmetry considerations, there will be a nonzero matrix element for scattering energy from the zero wave vector FMR mode of  $m = 1$  character, to  $m = 1$  modes of finite wave vector on the FMR branch which are degenerate with the FMR mode. We see when Eq. (6a) is

supplemented by an exchange term that scales as  $Dk^2$ , there is always a minimum in the dispersion relation of  $m=1$  spin waves away from zero wave vector, and thus there always will be finite wave vector modes degenerate with the FMR mode. However, when  $R < R_C = (D/\pi M_S)^{1/2}$ , from the structure of the dispersion curve the minimum will lie quite near zero wave vector, and the number of degenerate modes will be rather small. When  $R > R_C$ , the minimum will be in the vicinity of  $k = 1/R$ , and we expect the mechanism to be more efficient. For Ni,  $R_C$  is roughly 100 Å, and for Fe perhaps a factor of 2 shorter.

If the surface has, say, roughness of random character, so that azimuthal symmetry is no longer present, then the matrix element for scattering energy from the  $m=1$  FMR mode to modes with  $m > 1$  is nonzero. The criterion  $R > R_C$  remains relevant, in that it is for these larger radii that the dispersion relation for the  $m > 1$  magnetostatic modes (those which approach the FMR frequency as the wave vector vanishes) has an off center minimum. Also, this is a crude criterion for the appearance of zero wave vector modes below the FMR frequency of the cylinder, which is another source of finite wave vector modes degenerate with the FMR mode.

The above discussion suggests that the two magnon mechanism should be relatively inefficient in very small radius nanowires with  $R < R_C$ , but for larger nanowires we suggest it should be quite efficient. A detailed theory, beyond the scope of the present paper, will be required to explore this question further.

Another aspect of the geometry considered here is the large microwave magnetic field created outside the wire, by the precession of the magnetization. We see from Eq. (18) that for a spin wave with finite wave  $k$ , we have a field that falls off as  $\exp(-\kappa\rho)/\rho^{1/2}$  far from the wire. For long wavelength modes, this field has a very long range. In the limit of zero wave vector, we see from Eqs. (36) that the field created by the precession of the magnetization falls off inversely with the square of the distance from the center of the wire. The existence of this large field outside the nanowire is a substantial difference that the situation with thin films. If, for

the thin film, we consider the uniform precession mode excited in an FMR experiment, the macroscopic magnetic field created by precession of the magnetization is completely confined to within the film. There are “magnetic poles” on the film surfaces associated with the precessing magnetization, but the field generated by these is confined to within the film itself, as in a condenser plate problem. If we consider a spin wave whose wave vector parallel to the film surfaces is  $k$ , there is a macroscopic field outside with the spatial variation  $\exp(-kz)$  if the film surfaces are parallel to the  $xy$  plane, but the prefactor which controls the strength of this field scales as  $4\pi M_S(kd)$ , where  $d$  is the film thickness. This field is thus very weak in the thin film limit, or whenever the wavelength of the spin wave is large compared to the film thickness.

The existence of these large fields outside the nanowire have interesting implication for samples such as those explored by the authors of Ref. 1. We have long ranged interactions between the nanowires, so one is led to explore the collective excitations of the nanowire array. In the particular case of the samples used by Ebels and Wigen, the nanowires are accurately parallel to each other, but randomly arrayed over a plane. We thus have a random two-dimensional (2D) system with long ranged interactions. Indeed, if one were to excite spin waves of variable wavelength  $k$ , as in a light scattering experiment, then the ratio of the average interwire separation to the range of interaction can be varied. There is an analogy between this system, and the vortex glass state of 2D superconductors, where here the average vortex separation can be varied, but the range of the interaction if fixed as the London penetration depth. In the case of nanowire arrays, the nature of their collective excitations will be a most interesting topic, for ordered and disordered arrays.

#### ACKNOWLEDGMENTS

This research was stimulated by conversations with Dr. Ursula Ebels and Professor P. E. Wigen. Support was provided by the U.S. Army Research Office (Durham), under Contract No. CS0001028.

<sup>1</sup>U. Ebels and P. E. Wigen (unpublished).

<sup>2</sup>See the discussion that begins on p. 348 of the chapter by L. R. Walker, in *Magnetism*, edited by G. Rado and H. Suhl (Academic Press, New York, 1963), Vol. 1.

<sup>3</sup>B. C. Fletcher and C. Kittel, *Phys. Rev.* **120**, 2004 (1960).

<sup>4</sup>Lai Wu-Yan, Wang Ding-Sheng, and Pu Fu-Cho, *Acta Phys. Sin.* **26**, 285 (1977).

<sup>5</sup>R. P. Erickson and D. L. Mills, *Phys. Rev. B* **43**, 10 715 (1991).

<sup>6</sup>Rodrigo Arias and D. L. Mills, *Phys. Rev. B* **60**, 7395 (1999).

<sup>7</sup>A. Azevedo, A. B. Oliveira, F. M. de Aguiar, and S. M. Rezende, *Phys. Rev. B* **62**, 5331 (2000).

<sup>8</sup>S. O. Demokritov and B. Hillebrands, *J. Magn. Magn. Mater.* **200**, 706 (1999).

<sup>9</sup>For a recent discussion of this effect, and its influence on the response characteristics of device structures, see R. E. Camley and D. L. Mills, *J. Appl. Phys.* **82**, 3058 (1997).